

# Moveout inversion of $P$ -wave data for horizontal transverse isotropy

Pedro Contreras<sup>\*</sup>, Vladimir Grechka<sup>†</sup>, and Ilya Tsvankin<sup>†</sup>

<sup>\*</sup> *INTEVEP (Research Center of the Venezuelan Oil Company), Apartado 76343, Caracas 1070A, Venezuela*

<sup>†</sup> *Center for Wave Phenomena, Colorado School of Mines, Golden, CO 80401-1887*

## ABSTRACT

The transversely isotropic model with a horizontal symmetry axis (HTI media) has been extensively used in seismological studies of fractured reservoirs. Here, we apply to horizontal transverse isotropy a parameter estimation technique developed by Grechka and Tsvankin for the more general orthorhombic media. Our methodology is based on the inversion of azimuthally-dependent  $P$ -wave normal-moveout (NMO) velocities from horizontal and dipping reflectors.

NMO velocity for a given reflection event represents an ellipse determined by three combinations of the medium parameters. The NMO ellipses from horizontal reflectors can be inverted for the azimuth  $\beta$  of the horizontal symmetry axis, the vertical velocity  $V_{P0}$ , and the Thomsen-type anisotropic parameter  $\delta^{(V)}$ . We describe a method for obtaining the remaining (for  $P$ -waves) anisotropic parameter  $\eta^{(V)}$  (or  $\epsilon^{(V)}$ ) from the NMO ellipse corresponding to a dipping reflector of arbitrary azimuth. Then these anisotropic coefficients can be combined to evaluate the crack density and predict whether the cracks are fluid-filled or dry. Although estimation of  $\eta^{(V)}$  can be carried out using the general algorithm developed for orthorhombic media, we show that higher stability may be achieved by assuming the HTI model from the outset of the inversion procedure.

To recover the interval parameters of vertically inhomogeneous HTI media, we apply the generalized Dix equation that operates with the  $2 \times 2$  symmetric matrices representing NMO ellipses. Our algorithm is designed to find the interval values of  $\beta$ ,  $V_{P0}$ ,  $\epsilon^{(V)}$ , and  $\delta^{(V)}$  using moveout from horizontal and dipping reflectors measured at different vertical times. We apply our method to a multi-azimuth  $P$ -wave data set generated by ray tracing for a layered HTI medium with depth-varying orientation of the symmetry axis and confirm the high stability of the inversion procedure.

A unique feature of the HTI model that distinguishes it from both vertical transverse isotropy and orthorhombic media is that moveout inversion provides not just zero-dip NMO velocities and anisotropic coefficients, but also the true vertical velocity. As a result, reflection  $P$ -wave data acquired over HTI formations contain enough information for anisotropic *depth* processing.

**Key words:** HTI media, NMO ellipse, generalized Dix equation

## Introduction

Horizontal transverse isotropy (Figure 1) is a common model in shear-wave studies of fractured reservoirs that describes a system of parallel vertical penny-shaped

cracks embedded in an isotropic host rock (e.g., Thomsen, 1988). The fractional difference between the velocities of split  $S$ -waves at vertical incidence gives a good estimate of the crack density and, therefore, provides an important insight into the physical properties of the frac-

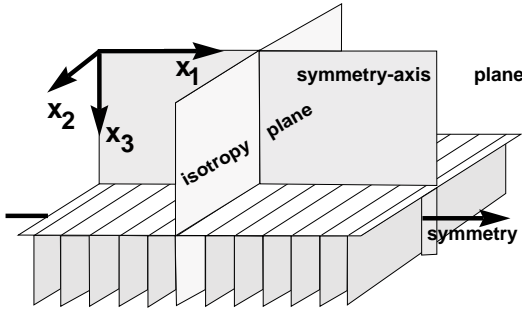


**Figure 1.** HTI model is used to describe a system of parallel vertical cracks in an isotropic background medium. The symmetry axis is orthogonal to the cracks; the plane parallel to the cracks is called the “isotropy plane.”

tured reservoir. An alternative approach to parameter estimation in HTI media, discussed by Tsvankin (1997), is based on the inversion of azimuthally dependent reflection traveltimes. Tsvankin (1997) gave an exact equation for normal-moveout (NMO) velocity of pure modes in a horizontal HTI layer and showed that it represents an ellipse with the axes parallel to the vertical symmetry planes of the medium. For  $P$ -waves, the NMO ellipse depends on the azimuth of the symmetry axis  $\beta$ , the vertical velocity  $V_{P0}$ , and the anisotropic coefficient  $\delta^{(V)}$  defined by analogy with Thomsen’s (1986) parameter  $\delta$  for TI models with a vertical symmetry axis (VTI media).  $P$ -wave kinematic signatures in HTI media are controlled by  $V_{P0}$ ,  $\delta^{(V)}$  and another anisotropic coefficient,  $\epsilon^{(V)}$ , that is close to the fractional difference between the symmetry-direction velocity and  $V_{P0}$ . Tsvankin (1997) suggested to obtain  $\epsilon^{(V)}$  either by combining NMO velocities of the  $P$ -wave and slow  $S$ -wave or by inverting dip-dependent  $P$ -wave moveout in the vertical plane that contains the symmetry axis (the “symmetry-axis plane”). Note that the inversion of dip moveout proposed by Tsvankin is based on his 2-D NMO equation (Tsvankin, 1995) and, therefore, can be applied only if the dip plane of the reflector contains the symmetry axis. The parameter  $\epsilon^{(V)}$  can also be recovered from nonhyperbolic (long-spread) moveout described by Al-Dajani and Tsvankin (1996). The set of the three  $P$ -wave moveout coefficients ( $V_{P0}$ ,  $\delta^{(V)}$ ,  $\epsilon^{(V)}$ ) can be used to reconstruct  $P$ -wave phase velocity, as well as estimate the crack density and investigate the contents of the fracture network (Tsvankin, 1997; Rüger, 1996).

Here, we generalize the previous parameter-estimation results by presenting an algorithm that operates with azimuthally-dependent NMO velocity from a dipping reflector with arbitrary orientation. As shown by

Grechka and Tsvankin (1996), the azimuthal variation of pure-mode NMO velocity typically represents an ellipse for any inhomogeneous arbitrary anisotropic medium. Since the ellipse is fully described by three quantities (e.g., by its orientation and the lengths of the semi-axes), only three combinations of medium parameters can be found from multi-azimuth NMO velocity measurements of a certain mode at a given spatial location. Clearly, these parameter combinations depend on the type of anisotropic model for which the inversion is carried out. For example, Grechka and Tsvankin (1996) proved that the  $P$ -wave NMO ellipse in VTI media, expressed through the horizontal slowness components of the zero-offset ray, is a function of two Alkhalifah-Tsvankin (1995) parameters: the “zero-dip” NMO velocity from a horizontal reflector  $V_{\text{nmo}}(0)$  and the “anellipticity” coefficient  $\eta$ . For the more complicated azimuthally-anisotropic model with orthorhombic symmetry, NMO velocity of  $P$ -waves depends on six quantities: the azimuth of one of the vertical symmetry planes, the zero-dip NMO velocities in the symmetry-plane directions  $V_{\text{nmo}}^{(1,2)}$  and three coefficients  $\eta^{(1,2,3)}$  defined similarly to the parameter  $\eta$  for VTI media. Grechka and Tsvankin (1997), who obtained this result, also developed a parameter-estimation procedure designed to find the symmetry-plane orientation and the five moveout parameters from the NMO ellipses of a horizontal and a dipping event.

The method of Grechka and Tsvankin (1997) can be directly applied to the inversion of the azimuthally dependent NMO velocity in HTI media because horizontal transverse isotropy can be considered as a special case of the general orthorhombic model. The transition from orthorhombic to HTI media becomes particularly simple within the framework of Tsvankin’s (1996) notation for orthorhombic anisotropy. For instance, the  $P$ -wave NMO ellipse from a horizontal reflector in HTI media (Tsvankin, 1997) can be obtained from the corresponding NMO ellipse in orthorhombic media (Grechka and Tsvankin, 1996) just by setting the appropriate  $\delta$  coefficient to zero. Likewise, the  $P$ -wave NMO velocity of dipping events in HTI media depends on only one  $\eta$  coefficient ( $\eta^{(V)}$ ) directly related to the parameter  $\epsilon^{(V)}$ . Since the NMO ellipse from a dipping reflector generally provides us with three independent equations, we have useful redundancy in estimating  $\eta^{(V)}$ . Hence, the inversion for  $\eta^{(V)}$  in HTI media is expected to be more stable than that for the three coefficients  $\eta^{(1,2,3)}$  in orthorhombic media.

To extend the moveout-inversion algorithm to vertically-inhomogeneous HTI media with arbitrary azimuth of the symmetry axis in each layer, we use the generalized Dix equation of Grechka et al. (1997). This

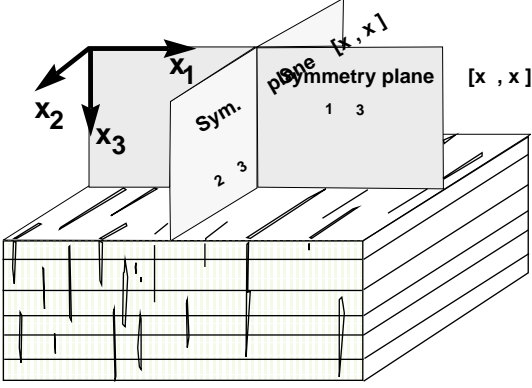


**Figure 2.** Orthorhombic media have three mutually orthogonal planes of mirror symmetry. One of the reasons for orthorhombic anisotropy is a combination of parallel vertical cracks and vertical transverse isotropy in the background medium.

equation expresses the exact NMO velocity for a stack of layers above a dipping reflector as an average of the matrices responsible for the interval NMO ellipses. Dix-type differentiation allows us to find the interval values of  $\beta$ ,  $V_{P0}$ ,  $\delta^{(V)}$ , and  $\epsilon^{(V)}$ , which are sufficient to perform *depth* processing in HTI media. We also compare the performance of the moveout inversion technique for HTI and orthorhombic media and present a numerical test of our parameter-estimation methodology for a stratified HTI model.

### Notation for HTI and Orthorhombic Media

Since our approach is based on adapting the methodology of Grechka and Tsvankin (1997) developed for orthorhombic media, we need to review the relation between the parameters of orthorhombic and HTI models. Orthorhombic (or orthotropic) symmetry system may be caused, for instance, by a set of parallel vertical cracks embedded in a background VTI medium (Figure 2) or by two orthogonal vertical crack systems in a purely isotropic or VTI matrix (e.g., Wild and Crampin, 1991; Schoenberg and Helbig, 1997). Regardless of the reasons for orthorhombic anisotropy, it is characterized by three mutually orthogonal planes of mirror symmetry, which are conventionally chosen as the coordinate planes. Tsvankin (1996) used the fact that the Christoffel equation has an identical form within the symmetry planes of orthorhombic and VTI media to parameterize orthorhombic models by two vertical velocities (the “isotropic” quantities) and seven dimensionless anisotropic coefficients. This notation, based on the same principle as Thomsen parameters for VTI media, is particularly

convenient for traveltime inversion (Grechka and Tsvankin, 1997). The expressions for Tsvankin’s parameters in terms of the stiffness coefficients  $c_{ij}$  and density  $\rho$  are given below.

- $V_{P0}$  –  $P$ -wave vertical velocity:

$$V_{P0} \equiv \sqrt{\frac{c_{33}}{\rho}}. \quad (1)$$

- $V_{S0}$  – the vertical velocity of the  $S$ -wave polarized in the  $x_1$ -direction:

$$V_{S0} \equiv \sqrt{\frac{c_{55}}{\rho}}. \quad (2)$$

- $\epsilon^{(2)}$  – the VTI parameter  $\epsilon$  in the  $[x_1, x_3]$  symmetry plane normal to  $x_2$ -axis (this explains the superscript “2”):

$$\epsilon^{(2)} \equiv \frac{c_{11} - c_{33}}{2 c_{33}}. \quad (3)$$

- $\delta^{(2)}$  – the VTI parameter  $\delta$  in the  $[x_1, x_3]$  plane:

$$\delta^{(2)} \equiv \frac{(c_{13} + c_{55})^2 - (c_{33} - c_{55})^2}{2 c_{33} (c_{33} - c_{55})}. \quad (4)$$

- $\gamma^{(2)}$  – the VTI parameter  $\gamma$  in the  $[x_1, x_3]$  plane :

$$\gamma^{(2)} \equiv \frac{c_{66} - c_{44}}{2 c_{44}}. \quad (5)$$

- $\epsilon^{(1)}$  – the VTI parameter  $\epsilon$  in the  $[x_2, x_3]$  symmetry plane:

$$\epsilon^{(1)} \equiv \frac{c_{22} - c_{33}}{2 c_{33}}. \quad (6)$$

- $\delta^{(1)}$  – the VTI parameter  $\delta$  in the  $[x_2, x_3]$  plane:

$$\delta^{(1)} \equiv \frac{(c_{23} + c_{44})^2 - (c_{33} - c_{44})^2}{2 c_{33} (c_{33} - c_{44})}. \quad (7)$$

- $\gamma^{(1)}$  – the VTI parameter  $\gamma$  in the  $[x_2, x_3]$  plane:

$$\gamma^{(1)} \equiv \frac{c_{66} - c_{55}}{2 c_{55}}. \quad (8)$$

- $\delta^{(3)}$  – the VTI parameter  $\delta$  in the  $[x_1, x_2]$  plane ( $x_1$  plays the role of the symmetry axis):

$$\delta^{(3)} \equiv \frac{(c_{12} + c_{66})^2 - (c_{11} - c_{66})^2}{2 c_{11} (c_{11} - c_{66})}. \quad (9)$$

An important parameter combination that we will use below is the shear-wave splitting coefficient at vertical incidence:

$$\gamma^{(S)} \equiv \frac{c_{44} - c_{55}}{2 c_{55}} = \frac{\gamma^{(1)} - \gamma^{(2)}}{1 + 2\gamma^{(2)}}. \quad (10)$$

Only a subset of these parameters ( $V_{P0}$ ,  $\epsilon^{(1,2)}$ , and  $\delta^{(1,2,3)}$ ) control  $P$ -wave kinematic signatures for orthorhombic media (Tsvankin, 1996). Furthermore, Grechka and Tsvankin (1997) showed that  $P$ -wave

normal-moveout velocity, expressed through the horizontal slowness components of the zero-offset ray, depends on just five parameters – the symmetry-plane NMO velocities from a horizontal reflector

$$V_{\text{nmo}}^{(i)} = V_{P0} \sqrt{1 + 2 \delta^{(i)}}, \quad (i = 1, 2) \quad (11)$$

and three anisotropic coefficients  $\eta^{(1,2,3)}$  defined by analogy with the parameter  $\eta$  (Alkhalifah and Tsvankin, 1995) in VTI media:

- $\eta^{(2)}$  – the VTI parameter  $\eta$  in the vertical symmetry plane  $[x_1, x_3]$ :

$$\eta^{(2)} = \frac{\epsilon^{(2)} - \delta^{(2)}}{1 + 2 \delta^{(2)}}. \quad (12)$$

- $\eta^{(1)}$  – the VTI parameter  $\eta$  in the vertical symmetry plane  $[x_2, x_3]$ :

$$\eta^{(1)} = \frac{\epsilon^{(1)} - \delta^{(1)}}{1 + 2 \delta^{(1)}}. \quad (13)$$

- $\eta^{(3)}$  – the VTI parameter  $\eta$  in the horizontal symmetry plane  $[x_1, x_2]$  ( $x_1$  plays the role of the symmetry axis):

$$\eta^{(3)} = \frac{\epsilon^{(1)} - \epsilon^{(2)} - \delta^{(3)}(1 + 2\epsilon^{(2)})}{(1 + 2\epsilon^{(2)})(1 + 2\delta^{(3)})}. \quad (14)$$

For the HTI model that may be considered as a special case of orthorhombic media, the number of independent parameters reduces from nine to five. If we align the symmetry axis with the  $x_1$ -direction (Figure 1), the velocities of all three modes in the  $[x_2, x_3]$ -plane (the isotropy plane) become constant, and the anisotropic coefficients in this plane [equations (6) – (8)] go to zero (Tsvankin, 1996):

- $\epsilon^{(1)} = 0,$  (15)

- $\delta^{(1)} = 0,$  (16)

- $\gamma^{(1)} = 0.$  (17)

Since the symmetry-axis plane  $[x_1, x_3]$  of HTI media is equivalent to the orthorhombic  $[x_1, x_3]$  symmetry plane, the definitions of the anisotropic coefficients  $\epsilon^{(2)}$ ,  $\delta^{(2)}$ , and  $\gamma^{(2)}$  [equations (3) – (5)] remain valid for horizontal transverse isotropy. Tsvankin (1997) and Rüger (1996), who introduced Thomsen-style parameterization for HTI media, called these parameters  $\epsilon^{(V)}$ ,  $\delta^{(V)}$ , and  $\gamma^{(V)}$ , respectively:

- $\epsilon^{(V)} \equiv \epsilon^{(2)},$  (18)

- $\delta^{(V)} \equiv \delta^{(2)},$  (19)

- $\gamma^{(V)} \equiv \gamma^{(2)}.$  (20)

The coefficient  $\delta^{(3)}$  [equation (9)] for HTI media becomes a function of  $\epsilon^{(V)}$ ,  $\delta^{(V)}$  and the ratio of the vertical velocities (Tsvankin, 1997):

$$\delta^{(3)} = \frac{\delta^{(V)} - 2\epsilon^{(V)}(1 + \epsilon^{(V)}/f)}{(1 + 2\epsilon^{(V)}/f)(1 + 2\delta^{(V)})}, \quad (21)$$

where

$$f = 1 - V_{S0}^2/V_{P0}^2. \quad (22)$$

Thus, properties of an HTI medium are determined by a total of five independent parameters –  $V_{P0}$ ,  $V_{S0}$ ,  $\epsilon^{(V)}$ ,  $\delta^{(V)}$ , and  $\gamma^{(V)}$ . As demonstrated by Tsvankin (1997), kinematic signatures of  $P$ -waves can be described with sufficient accuracy by the vertical velocity  $V_{P0}$ ,  $\epsilon^{(V)}$ , and  $\delta^{(V)}$ . Hence, these three parameters are supposed to control  $P$ -wave NMO velocity as well. Indeed, the NMO velocities from a horizontal reflector in the symmetry planes [equation (11)] become

$$V_{\text{nmo}}^{(1)} = V_{P0}, \quad (23)$$

$$V_{\text{nmo}}^{(2)} = V_{P0} \sqrt{1 + 2 \delta^{(V)}}. \quad (24)$$

The number of independent  $\eta$  coefficients for HTI media reduces from three to one; in accordance with the definitions of  $\eta^{(1,2,3)}$  [equations (12)–(14)],

- $\eta^{(1)} = 0,$  (25)

- $\eta^{(2)} = \eta^{(V)} = \frac{\epsilon^{(V)} - \delta^{(V)}}{1 + 2 \delta^{(V)}},$  (26)

- $\eta^{(3)} = \frac{\epsilon^{(V)} - \delta^{(V)}}{1 + 2 (\delta^{(V)} + \epsilon^{(V)} \frac{1-f}{f})} \approx \eta^{(V)}.$  (27)

Although the shear-wave vertical velocity does enter equation (27) through the quantity  $f$ , its influence can be ignored. Note that if the symmetry axis points in the  $x_2$ -direction, then the parameter  $\eta^{(2)} = 0$ , while  $\eta^{(1)}$  and  $\eta^{(3)}$  become identical and equal to  $\eta^{(V)}$ . Therefore, instead of five moveout parameters in orthorhombic media, we have only three ( $V_{P0}$ ,  $\epsilon^{(V)}$  or  $\eta^{(V)}$ , and  $\delta^{(V)}$ ) in the HTI model.

## NMO Ellipses in a Homogeneous HTI Layer

Grechka and Tsvankin (1996) obtained a general equation for azimuthally-varying NMO velocity of any pure mode in the form

$$V_{\text{nmo}}^{-2}(\alpha) = W_{11} \cos^2 \alpha + 2W_{12} \sin \alpha \cos \alpha + W_{22} \sin^2 \alpha, \quad (28)$$

where  $\alpha$  is the azimuth of the common-midpoint (CMP) line with respect to the  $x_1$ -axis and the symmetric matrix  $\mathbf{W}$  is given by

$$W_{ij} = \tau_0 \frac{\partial p_i}{\partial x_j}, \quad (i, j = 1, 2). \quad (29)$$

Here,  $\tau_0$  is the one-way zero-offset traveltime and  $p_1$  and  $p_2$  are the horizontal components of the slowness vector for rays emanating from the zero-offset reflection point; the spatial derivatives of  $p_i$  are evaluated at the CMP

location. Equation (28) is valid for any inhomogeneous anisotropic medium in which reflection traveltime can be expanded in a Taylor series near the common midpoint. Grechka and Tsvankin (1996) showed that matrix  $\mathbf{W}$  is usually positive definite, and the azimuthally dependent NMO velocity (28) represents an ellipse in the horizontal plane. A more detailed description of the NMO ellipse can be found in Grechka and Tsvankin (1996) and Grechka et al. (1997); the latter paper also contains an explicit NMO expression for a homogeneous layer based on equation (28). Below, we use these results to discuss  $P$ -wave NMO velocity from horizontal and dipping reflectors in HTI media.

### Horizontal reflector

Suppose the symmetry axis of a horizontal HTI layer makes the angle  $\beta$  with the coordinate axis  $x_1$ . Adapting the exact expression for normal-moveout presented by Tsvankin (1997), we can represent the  $P$ -wave NMO ellipse as

$$\frac{1}{V_{\text{nmo}}^2(\alpha)} = \frac{\cos^2(\alpha - \beta)}{V_{P,\text{nmo}}^2} + \frac{\sin^2(\alpha - \beta)}{V_{P0}^2}, \quad (30)$$

where  $V_{P,\text{nmo}} \equiv V_{\text{nmo}}^{(2)} = V_{P0}\sqrt{1 + 2\delta^{(V)}}$  is the NMO velocity in the symmetry-axis plane given by equation (24). Equation (30) can also be obtained from the more general NMO equation in an orthorhombic layer (Grechka and Tsvankin, 1996) by setting the  $\delta$  coefficient in the isotropy plane to zero.

Clearly, the semi-axes of the ellipse (30) are aligned with the vertical symmetry planes of the HTI layer, and the NMO velocity is determined by three quantities: the azimuth  $\beta$  of the symmetry axis, the vertical velocity  $V_{P0}$ , and the anisotropic coefficient  $\delta^{(V)}$ . A minimum of three well-separated azimuthal moveout measurements are needed to reconstruct the NMO ellipse and find  $\beta$ ,  $V_{P0}$ , and  $\delta^{(V)}$ . Then we can use the vertical velocity to obtain the layer thickness

$$z = V_{P0}\tau_0, \quad (31)$$

where  $\tau_0$  is the one-way vertical traveltime.

The accuracy and stability of this inversion procedure, as well as the optimal number and spread of CMP lines is discussed in detail by Al-Dajani and Alkhalifah (1997). Note that unambiguous recovery of  $V_{P0}$  and  $\delta^{(V)}$  is impossible without identification of the symmetry-axis and isotropy planes, which cannot be done using moveout data alone. However, the parameter  $\delta^{(V)}$  is usually negative for fractured formations (Tsvankin, 1997) and, therefore, the smaller semi-axis of the NMO ellipse should correspond to the direction of the symmetry axis.

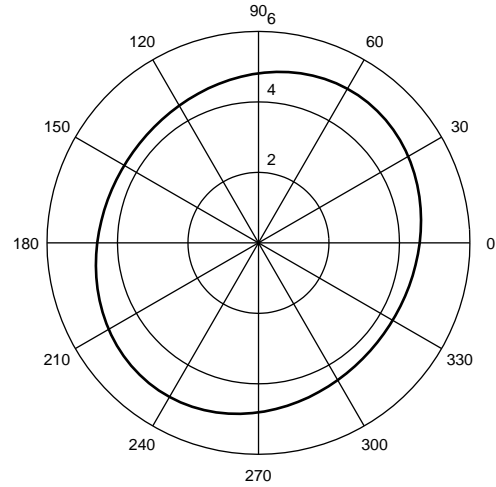


**Figure 3.** The  $P$ -wave NMO ellipse in an HTI layer above a dipping reflector. The reflector dip is equal to  $30^\circ$ , the azimuth of the dip plane is  $45^\circ$ . The medium parameters correspond to a system of fluid-filled cracks embedded in an isotropic matrix (Rüger, 1996):  $V_{P0} = 4.498$  km/s,  $V_{S0} = 2.53$  km/s,  $\epsilon^{(V)} = -0.003$ ,  $\delta^{(V)} = -0.088$ . The azimuth of the symmetry axis  $\beta = 0^\circ$ .

### Dipping reflector

Tsvankin (1997) discussed one special case of dip-moveout inversion in HTI media. If the dip plane of the reflector coincides with the symmetry-axis plane, the moveout problem on the dip line becomes two-dimensional because reflected rays do not deviate from the incidence plane. Due to the kinematic equivalence between the symmetry-axis plane of HTI media and any vertical plane in VTI media, the dip-dependence of the  $P$ -wave NMO velocity in the symmetry-axis plane is controlled by the parameter  $\eta^{(V)}$  exactly in the same way as  $\eta$  determines dip moveout in VTI media. This means that the dip-moveout inversion method of Alkhalifah and Tsvankin (1995) is fully applicable to the estimation of  $\eta^{(V)}$  in the symmetry-axis plane.

Here, we extend this result to a dipping reflector with arbitrary orientation by using the general NMO equation in homogeneous layer given by Grechka et al. (1997) and adapting the inversion methodology of Grechka and Tsvankin (1997) originally developed for orthorhombic media. If the reflector strike is not aligned with either of the symmetry-plane azimuths, the NMO ellipse cannot be represented in the simple form (30) since its semi-axes deviate from the symmetry planes. For instance, for a reflector with the dip plane making an angle of  $45^\circ$  with the symmetry axis (Figure 3), the azimuth of the largest semi-axis of the NMO ellipse is equal to  $55.6^\circ$ .

The NMO ellipse in Figure 3 was calculated using an exact equation of Grechka et al. (1997) who expressed

the components of the matrix  $\mathbf{W}$  [equation (29)] for a homogeneous layer through the slowness vector of the zero offset ray. This equation, valid for any pure mode and arbitrary orientation of the CMP line, has the following form:

$$V_{\text{nmo}}^{-2}(\alpha, p_1, p_2) = \frac{p_1 q_{,1} + p_2 q_{,2} - q}{q_{,11} q_{,22} - q_{,12}^2} [q_{,22} \cos^2 \alpha - 2 q_{,12} \sin \alpha \cos \alpha + q_{,11} \sin^2 \alpha], \quad (32)$$

where  $q \equiv q(p_1, p_2) \equiv p_3$  is the vertical component of the slowness vector;  $q_{,i}$  and  $q_{,ij}$ , ( $i, j=1,2$ ) denote the partial derivatives  $q_{,i} \equiv \partial q / \partial p_i$  and  $q_{,ij} \equiv \partial^2 q / \partial p_i \partial p_j$  that should be evaluated for the zero-offset ray. The horizontal slownesses ( $p_1, p_2$ ) for the zero-offset ray can be found from the reflection slopes on zero-offset sections recorded in two different azimuthal directions.

Equation (32) can be used to obtain the parameter  $\eta^{(V)}$  from the azimuthally dependent NMO velocity of an arbitrary dipping event. To gain analytic insight into this inversion procedure, we use the weak anisotropy approximation (linearization in the anisotropic coefficients) for the  $P$ -wave NMO ellipse in orthorhombic media derived by Grechka and Tsvankin (1997). After substituting the HTI relationships (23)–(27) into their equations (A-1) – (A-10), we find

$$\begin{aligned} V_{\text{nmo}}^{-2}(\alpha, p_1, p_2) &= \\ &= \cos^2 \alpha \left\{ \frac{1}{V_{P,\text{nmo}}^2} - p_1^2 - 2p_1^2 \eta^{(V)} d_1 \right\} \\ &- 2 \sin \alpha \cos \alpha p_1 p_2 \left\{ 1 - 8\eta^{(V)} p_1^2 V_{P0}^2 d_2 \right\} \\ &+ \sin^2 \alpha \left\{ \frac{1}{V_{P0}^2} - p_2^2 + 2\eta^{(V)} p_1^4 V_{P0}^2 d_3 \right\}, \quad (33) \end{aligned}$$

where

$$d_1 = 6 - 9p_1^2 V_{P0}^2 + 4p_1^4 V_{P0}^4,$$

$$d_2 = 1 - p_1^2 V_{P0}^2 - 2p_2^2 V_{P0}^2,$$

$$d_3 = 1 - 4p_2^2 V_{P0}^2;$$

$\alpha$  is the angle with the symmetry axis.

Suppose that the azimuth of the dip plane of the reflector coincides with the symmetry-axis plane of an HTI layer. Then the zero-offset ray is confined to the  $[x_1, x_3]$  plane ( $p_2 = 0$ ), and approximation (33) yields

$$\begin{aligned} V_{\text{nmo}}^{-2}(\alpha, p_1, p_2) &= \\ &= \cos^2 \alpha \left\{ \frac{1}{V_{P,\text{nmo}}^2} - p_1^2 - 2p_1^2 \eta^{(V)} d_1 \right\} \\ &+ \sin^2 \alpha \left\{ \frac{1}{V_{P0}^2} + 2\eta^{(V)} p_1^4 V_{P0}^2 d_3 \right\}. \quad (34) \end{aligned}$$

The dip-line NMO velocity ( $\alpha = 0$ ) in this case is identical to the corresponding VTI approximation given

in Alkhalifah and Tsvankin (1995) and discussed for HTI media by Tsvankin (1997). Provided the zero-dip NMO velocity in the symmetry-axis plane has been obtained from horizontal events,  $V_{\text{nmo}}(\alpha = 0, p_1)$  for a dipping event (a single  $p_1 \neq 0$ ) is sufficient to obtain  $\eta^{(V)}$ . Equation (34) also shows that the strike-line NMO velocity ( $\alpha = 90^\circ$ ) provides a useful redundancy in estimating  $\eta^{(V)}$ .

If the dip plane of the reflector represents the isotropy plane ( $p_1 = 0$ ),

$$V_{\text{nmo}}^{-2}(\alpha, p_1, p_2) = \frac{\cos^2 \alpha}{V_{P,\text{nmo}}^2} + \sin^2 \alpha \left\{ \frac{1}{V_{P0}^2} - p_2^2 \right\}. \quad (35)$$

Clearly,  $\eta^{(V)}$  has no influence on both semi-axes of the ellipse (35) and, therefore, cannot be found from moveout data. Therefore, we expect the inversion of  $\eta^{(V)}$  to be unstable if the reflector azimuth is close to the isotropy plane of the HTI model.

Another situation when  $\eta^{(V)}$  is not well constrained by dip moveout is when the reflector is close to horizontal and both slowness components  $p_1$  and  $p_2$  in equation (33) are small. Relevant quantitative estimates can be found in Alkhalifah and Tsvankin (1995) for VTI media and in Grechka and Tsvankin (1997) for orthorhombic anisotropy.

## Parameter Estimation in an HTI Layer

$P$ -wave normal-moveout velocity in HTI media, expressed by equation (32), depends on the symmetry-axis orientation  $\beta$ , the vertical velocity  $V_{P0}$ , and the anisotropic coefficients  $\epsilon^{(V)}$  (or  $\eta^{(V)}$ ) and  $\delta^{(V)}$ . Since one NMO ellipse generally depends on three parameter combinations, we need at least two NMO ellipses from reflectors of different dips and azimuths to carry out the inversion procedure. NMO ellipses of two reflection events provide six equations for four unknowns, which ensures a useful redundancy and helps to stabilize the parameter estimation. Note that in orthorhombic media we have two more unknowns (Grechka and Tsvankin, 1997) for the same number of equations, so the inversion procedure in HTI media is expected to be more stable compared to that for orthorhombic models.

In subsequent analysis, we assume that one of the reflectors is horizontal. Then the axis orientation  $\beta$ ,  $V_{P0}$ , and  $\delta^{(V)}$  can be found from the horizontal event, which leaves  $\eta^{(V)}$  or  $\epsilon^{(V)}$  as the only unknown to be obtained from the NMO ellipse of a dipping event. As mentioned above, the negative value of  $\delta^{(V)}$  allows us to distinguish between the azimuths of the symmetry-axis and isotropy planes: the smallest semi-axis of the NMO ellipse from a horizontal reflector defines the direction of the symmetry

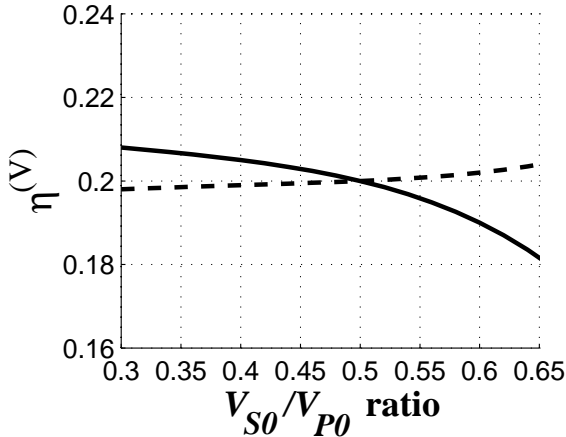


**Figure 4.** The influence of the shear-wave vertical velocity  $V_{S0}$  on the inversion for  $\eta^{(V)}$ . The azimuth of the dip plane of the reflector with respect to the symmetry axis is  $45^\circ$ , the dips are  $35^\circ$  (solid line) and  $70^\circ$  (dashed line). The medium parameters are  $V_{P0} = 4.0$  km/s,  $\epsilon^{(V)} = 0$ ,  $\delta^{(V)} = -0.143$ ,  $\eta^{(V)} = 0.2$ . The actual  $V_{S0}/V_{P0}$  ratio is shown on the plot; the inversion was always performed with  $V_{S0}/V_{P0} = 0.5$ .

axis (normal to the fractures). It may happen that  $\delta^{(V)} = 0$ , and the NMO ellipse of horizontal events degenerates into a circle. In this case, the azimuth  $\beta$  of the symmetry axis has to be retrieved, along with  $\eta^{(V)}$ , from the NMO velocity of a dipping event (then we have three equations for two unknowns).

Our inversion algorithm is based on the exact equation for the NMO ellipse (32) and uses the three components of the corresponding matrix  $\mathbf{W}$  as input data. Assuming that  $\beta$ ,  $V_{P0}$ , and  $\delta^{(V)}$  have already been found, we search for the value of  $\eta^{(V)}$  that minimizes the norm of the difference

$$\mathcal{F}(\eta^{(V)}) = \|\mathbf{W}_{\text{measur}} - \mathbf{W}_{\text{theor}}\| = \min \quad (36)$$

between the measured and theoretical (computed) matrices  $\mathbf{W}$  that define the NMO ellipse (32). More details about this procedure are given in Grechka and Tsvankin (1997).

Before discussing the inversion results, we verify whether the shear-wave vertical velocity  $V_{S0}$  can be ignored in the parameter-estimation procedure. In agreement with Tsvankin (1997), although  $V_{S0}$  [or the quantity  $f$  from equation (22)] does enter the exact phase-velocity equations for the  $P$ -wave, its influence on normal moveout is negligibly small (Figure 4). Therefore, in the examples below we use a “reasonable” value of the  $V_{S0}/V_{P0}$  ratio that does not necessarily correspond to the true shear-wave vertical velocity in the model.

If the inversion is performed on error-free data (as in Figure 4 for  $V_{S0}/V_{P0} = 0.5$ ), the value of  $\eta^{(V)}$  is found

with excellent accuracy. To evaluate the stability of the parameter-estimation procedure, we introduced errors in the symmetry-plane NMO velocities from a horizontal reflector (Figure 5). For each reflection event, we present two sets of the inversion results, one of which is computed for the HTI model, while the other is obtained under the assumption that the model is orthorhombic.

Assuming the medium to be HTI from the outset of the inversion procedure, we recover  $\eta^{(V)}$  (thin solid line) in a stable fashion for the reflectors with azimuths of  $20^\circ$  and  $45^\circ$  (Figure 5a–d; by the azimuth we mean the angle between the dip plane of the reflector and the symmetry axis). In accordance with the weak-anisotropy approximation discussed above, the inversion for  $\eta^{(V)}$  becomes less stable as the reflector azimuth approaches the isotropy plane (Figure 5e, f). The value of  $\eta^{(V)}$  in this case is especially sensitive to errors in the zero-dip NMO velocity in the symmetry-axis plane (Figure 5f). (A small deviation of  $\eta^{(V)}$  from the actual value even in the absence of errors is caused by the wrong value of the shear-wave vertical velocity intentionally used in the inversion.)

Since in field experiments we may not know the medium symmetry in advance, it is interesting to carry out the inversion of the NMO ellipse (computed for the actual HTI model) using the algorithm of Grechka and Tsvankin (1997) for the more general orthorhombic medium. In this case, we have to invert three components of the matrix  $\mathbf{W}$  for three unknown parameters –  $\eta^{(1)}$ ,  $\eta^{(2)}$ , and  $\eta^{(3)}$ . An accurate inversion procedure should yield the expressions for  $\eta^{(1,2,3)}$  valid in HTI media:  $\eta^{(2)} = \eta^{(V)}$  and  $\eta^{(1)} = 0$ . Also, for the model from Figure 5  $\epsilon^{(V)} = 0$  and, as follows from equation (27),  $\eta^{(3)} = \eta^{(V)}$  (in general, the last relationship is approximate). If the zero-dip NMO velocities are not distorted, we indeed obtain the values that almost satisfy these HTI constraints. The errors in input data, however, get “distributed” among the three  $\eta$  parameters, and it might be difficult to recognize the HTI model by examining the inversion results. For instance, if the reflector azimuth is equal to  $20^\circ$  (Figure 5a, b), the value of  $\eta^{(2)}$  stays close to  $\eta^{(V)}$ , but  $\eta^{(1)}$  and  $\eta^{(3)}$  show substantial variations under the influence of errors in  $V_{P0}$ . This result is in agreement with the conclusion of Grechka and Tsvankin (1997) that if the dip plane of the reflector is near the  $[x_1, x_3]$  symmetry plane, NMO velocity constrains the *difference* between  $\eta^{(1)}$  and  $\eta^{(3)}$ , but not the individual values of the coefficients. The HTI signature is most apparent in the inverted values for the reflector azimuth of  $45^\circ$  (Figure 5c, d), where  $\eta^{(1)} \approx 0$  and  $\eta^{(2)}$  does not deviate much from  $\eta^{(3)}$  for the whole range of errors in the zero-dip NMO velocities.

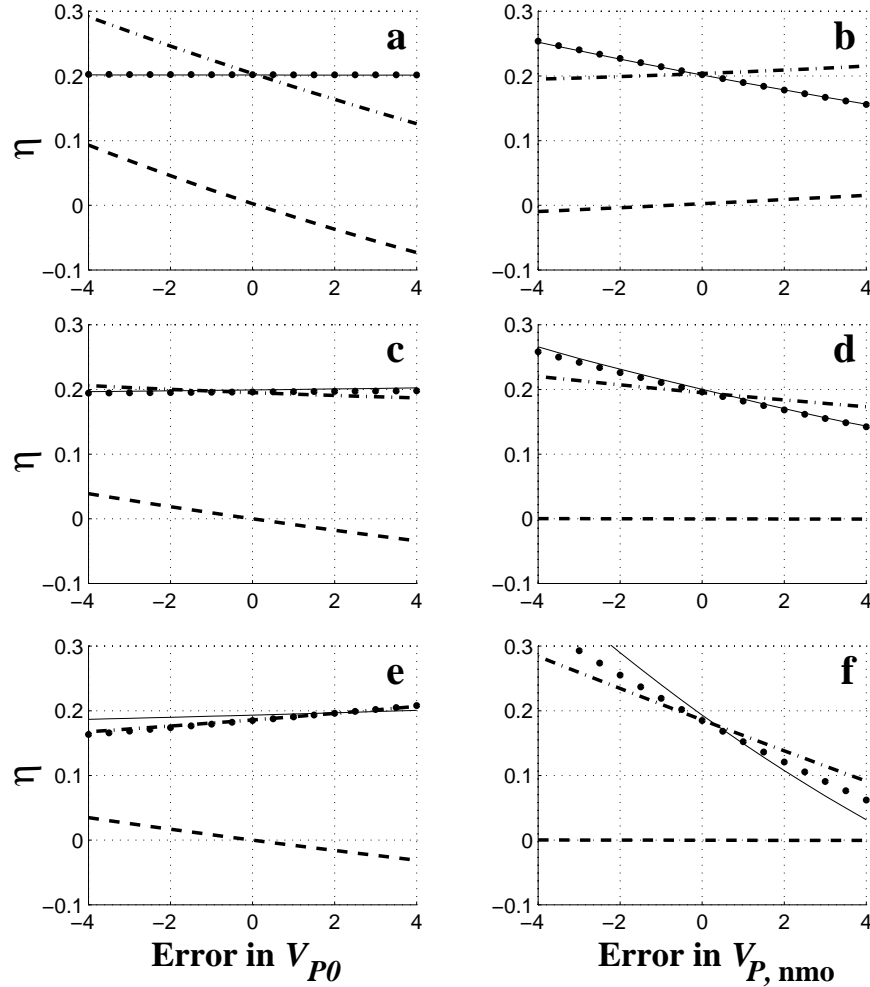


**Figure 5.** Inversion of the NMO ellipse for a dipping event in the presence of errors in the symmetry-plane NMO velocities from a horizontal reflector (in %). The reflector dip is  $50^\circ$ ; the azimuth of the dip plane is different for each row:  $20^\circ$  (a,b),  $45^\circ$  (c,d), and  $70^\circ$  (e,f). The layer parameters are  $V_{P0} = 4.0$  km/s,  $\epsilon^{(V)} = 0$ ,  $\delta^{(V)} = -0.143$ ,  $\eta^{(V)} = 0.2$ . The thin solid line denotes  $\eta^{(V)}$  obtained by assuming the HTI model in the inversion procedure. Under the assumption that the model is orthorhombic, we computed  $\eta^{(1)}$  (dashed),  $\eta^{(2)}$  (dotted), and  $\eta^{(3)}$  (dash-dotted).

### Moveout Inversion in Vertically Inhomogeneous HTI Media

The inversion approach described above can be extended to horizontally layered HTI media above a dipping reflector using the generalized Dix equation derived by Grechka et al. (1997). This equation expresses the exact effective NMO velocity in a stratified medium through the average of the matrices  $\mathbf{W}$  responsible for the interval NMO ellipses [equations (28) and (29)]:

$$\mathbf{W}^{-1}(L) = \frac{1}{\tau(L)} \sum_{\ell=1}^L \tau_\ell \mathbf{W}_\ell^{-1}, \quad (37)$$

where  $\mathbf{W}(L)$  and  $\mathbf{W}_\ell$  define the effective and interval NMO ellipses, respectively,  $\tau_\ell$  are the interval zero-offset

traveltimes, and  $\tau(L) = \sum_{\ell=1}^L \tau_\ell$ . Equation (37) is valid for reflections from a dipping interface beneath an arbitrary anisotropic vertically inhomogeneous overburden. Rewriting equation (37) in the differentiation form yields

$$\mathbf{W}_\ell^{-1} = \frac{\tau(\ell)\mathbf{W}^{-1}(\ell) - \tau(\ell-1)\mathbf{W}^{-1}(\ell-1)}{\tau(\ell) - \tau(\ell-1)}. \quad (38)$$

It should be emphasized that the interval matrices  $\mathbf{W}_\ell$  are evaluated for the horizontal slownesses  $p_1$  and  $p_2$  of the zero-offset ray and, therefore, generally do not correspond to physically existing reflectors in each layer. Therefore, equation (38) should be applied through a layer-stripping procedure that involves computation of the interval matrices  $\mathbf{W}_\ell$  and the interval zero-offset

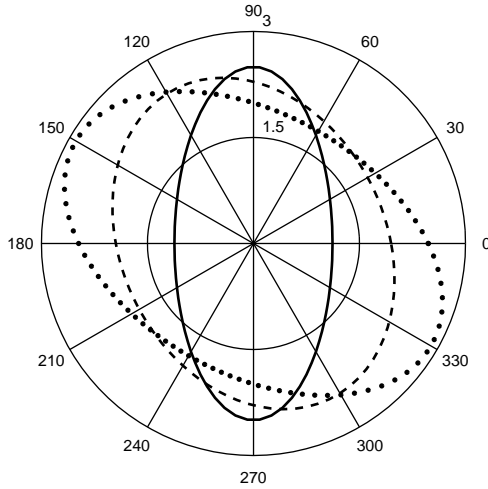


**Figure 6.** Azimuthally-dependent NMO velocities in an HTI model consisting of two horizontal layers. Solid line – the NMO ellipse from the bottom of the first layer; dotted – the interval ellipse for the second layer; dashed – the effective ellipse from the bottom of the second layer. The relevant parameters of the first layer are  $V_{P0,1} = 2.5$  km/s,  $\delta_1^{(V)} = -0.4$ ,  $\beta_1 = 0^\circ$ ,  $z_1 = 1.0$  km; for the second layer,  $V_{P0,2} = 2.9$  km/s,  $\delta_2^{(V)} = -0.3$ ,  $\beta_2 = 60^\circ$ ,  $z_2 = 1.0$  km.

traveltimes for the slowness components of the zero-offset ray.

Figure 6 illustrates the difference between the (exact) averaging of NMO ellipses and conventionally used (approximate) rms averaging of NMO velocities. The interval NMO ellipse for the second layer (dotted) was correctly restored by applying equation (38) to the effective NMO ellipses for the reflections from the top (solid) and bottom (dashed) of the layer. Note that at azimuth  $69^\circ$ , where two effective ellipses intersect and the effective NMO velocities are equal to each other, the interval NMO velocity in the second layer is *smaller* than both effective ones. This interval velocity would be *overestimated* by the conventional Dix differentiation of the NMO velocities at this azimuth. Likewise, the interval NMO ellipses intersect at an azimuth of  $61^\circ$ , where the effective NMO ellipse computed from equation (37) yields a *greater* effective NMO velocity than both interval values. In such a case, as discussed by Grechka and Tsvankin (1997), conventional Dix averaging *underestimates* the effective NMO velocity. A more detailed comparison of the exact NMO equation (37) and the rms averaging of NMO velocities is given in Grechka et al. (1997).

Here, we use a simple modification of the layer-stripping algorithm developed by Grechka and Tsvankin (1997) for orthorhombic media.

## Synthetic Example

To demonstrate the performance of our parameter-estimation methodology, we apply it to the inversion of ray-traced traveltimes in a stratified HTI model with a dipping reflector cutting through all layers. We computed the exact  $P$ -wave reflection traveltimes from horizontal and dipping reflectors along 6 azimuths with an increment of  $30^\circ$ . Large offsets were muted out to maintain the spreadlength-to-depth ratio of 1 for all reflections. Using the conventional hyperbolic approximation for reflection moveout, we calculated the best-fit moveout velocities at each azimuth and reconstructed the corresponding NMO ellipses. After carrying out the moveout inversion in the first layer, we used the generalized Dix equation (38) to recover the interval NMO ellipses for the horizontal and dipping events in the second layer and obtain the layer parameters. Then we repeated this operation for the last (third) layer; the inversion results along with the model parameters are given in Table 1. The maximum error in the interval vertical velocity  $V_{P0}$  and the layer thicknesses  $z$  is just 0.6%, while the errors in the interval anisotropic coefficients  $\epsilon^{(V)}$  and  $\delta^{(V)}$  are limited by 0.03. The orientation of the symmetry axis, which varied with depth, was accurately restored as well. The inversion errors are entirely due to the influence of nonhyperbolic moveout on the NMO velocities, which served as input data for parameter estimation. However, our results indicate that  $P$ -wave reflection moveout on conventional offsets close to the reflector depth does not deviate much from a hyperbola. The same conclusion was drawn by Grechka and Tsvankin (1997) in their study of reflection moveout in orthorhombic media.

## Physical properties of cracks from moveout inversion

The azimuthal variation of NMO velocity helps to determine the direction of the symmetry axis and, therefore, identify the fracture orientation. Also, the results of moveout inversion for HTI media can be directly related to the physical properties of crack systems important in characterization of fractured reservoirs. One of these properties is the crack density (the product of the number of cracks per unit volume and their mean cubed diameter), which is close to the shear-wave splitting parameter  $\gamma^{(S)}$  at vertical incidence (Thomsen, 1995). While  $P$ -wave moveout inversion cannot yield the shear-wave splitting parameter directly,  $\gamma^{(S)}$  [equation (10)] can be calculated from  $\epsilon^{(V)}$  and  $\delta^{(V)}$  using the constraint on the stiffness coefficients for the HTI model due to thin parallel cracks (Tsvankin, 1997):

Layer	Correct values					Inverted values				
	$z$ (km)	$V_{P0}$ (km/s)	$\epsilon^{(V)}$	$\delta^{(V)}$	$\beta$ (degrees)	$z$ (km)	$V_{P0}$ (km/s)	$\epsilon^{(V)}$	$\delta^{(V)}$	$\beta$ (degrees)
1	1.000	2.500	-0.100	-0.200	0.00	0.994	2.485	-0.130	-0.178	0.07
2	0.700	2.900	-0.050	-0.100	20.00	0.701	2.902	-0.040	-0.090	19.23
3	0.300	3.200	-0.200	-0.300	40.00	0.301	3.206	-0.181	-0.289	40.05

**Table 1.** Comparison of the actual and inverted parameters for a three-layer HTI model with a throughgoing dipping reflector. The reflector dip is  $40^\circ$ , the azimuth of the dip plane is  $60^\circ$ . The spreadlength-to-depth ratio is equal to unity for all events.

$$\gamma^{(S)} = \frac{V_{P0}^2}{2V_{S0}^2} \frac{\epsilon^{(V)} [2 - 1/f] - \delta^{(V)}}{1 + 2\epsilon^{(V)}/f + \sqrt{1 + 2\delta^{(V)}/f}}. \quad (39)$$

Although equation (39) involves the shear-wave vertical velocity that cannot be obtained from  $P$ -wave moveout data, a rough estimate of  $V_{S0}/V_{P0}$  is sufficient for applying this expression for  $\gamma^{(S)}$  in detecting “sweet spots” of high crack density.

Once the set of all three anisotropic coefficients ( $\gamma^{(S)}$ ,  $\epsilon^{(V)}$ , and  $\delta^{(V)}$ ) has been recovered, it can be used to deduce more information about the properties of the crack system. For instance, for thin fluid-filled cracks in the absence of equant porosity,  $\epsilon^{(V)} \approx 0$ , while  $\gamma^{(S)} \approx -\delta^{(V)}$  (Tsvankin, 1997). In contrast, for dry cracks typically  $\epsilon^{(V)} \approx \delta^{(V)} < 0$ , and  $|\epsilon^{(V)}|$  is much larger than  $\gamma^{(S)}$  (Rüger, 1996).

## Discussion and Conclusions

Normal-moveout velocity of  $P$  waves for horizontal transverse isotropy is controlled by the azimuth of the symmetry axis  $\beta$  (normal to the fractures), the vertical velocity  $V_{P0}$ , and the anisotropic coefficients  $\epsilon^{(V)}$  and  $\delta^{(V)}$ . For purposes of moveout inversion,  $\epsilon^{(V)}$  is convenient to replace with the “anellipticity” coefficient  $\eta^{(V)}$  responsible for dip moveout. Here, we show that all four parameters can be recovered in a stable fashion using azimuthally dependent NMO velocities from a horizontal and a dipping reflector. The NMO ellipse for a horizontal event can be inverted for the symmetry-axis orientation,  $V_{P0}$ , and  $\delta^{(V)}$  (Tsvankin, 1997), while the remaining coefficient,  $\eta^{(V)}$ , can be obtained from the moveout for a dipping reflector. In the case when  $\delta^{(V)} = 0$ , the NMO velocity from a horizontal reflector is independent of azimuth, and the angle  $\beta$  should be recovered (along with  $\eta^{(V)}$ ) from the NMO ellipse of a dipping event.

Our inversion algorithm is based on the exact NMO equation for a homogeneous layer of arbitrary symmetry given by Grechka et al. (1997) and follows the methodology developed by Grechka and Tsvankin (1997) for the more general orthorhombic model. In principle, it is pos-

sible to carry out the inversion assuming that the model is orthorhombic and identify the HTI symmetry by the specific relationships between the obtained  $\eta$  coefficients. Although this approach works well on error-free data, it can break down in field applications because the errors in input information tend to be distributed among the three orthorhombic  $\eta$  parameters in a complicated fashion. Therefore, to increase the stability of the inversion procedure, it is preferable to *assume* the HTI symmetry rather than deduce it from the inversion results.

The parameter  $\eta^{(V)}$  can be recovered with good accuracy for a wide range of reflector dips and azimuths, and is especially well-determined if the dip plane of the reflector is close to the direction of the symmetry axis. The only range of reflector azimuths unfavorable for  $\eta^{(V)}$  inversion corresponds to a vicinity of the isotropy plane.

We also extended our inversion technique to vertically inhomogeneous HTI media above an arbitrary oriented dipping reflector. This algorithm is based on the generalized Dix formula of Grechka et al. (1997) that operates with  $2 \times 2$  matrices responsible for the interval NMO ellipses evaluated at the horizontal slowness components of the zero-offset ray. As a result of this Dix-type differentiation procedure, we obtain the interval values of  $\beta$ ,  $V_{P0}$ ,  $\eta^{(V)}$  ( $\epsilon^{(V)}$ ),  $\delta^{(V)}$ , and the interval thickness  $z$ . Application of the Dix differentiation imposes obvious restrictions on the thickness of the interval, which are well known for isotropic media and remain valid in the presence of anisotropy.

The inversion algorithm was tested on ray-traced traveltimes data generated for a stratified HTI model with depth-varying orientation of the symmetry axis. All interval values were restored with excellent accuracy, which indicates that nonhyperbolic moveout does not seriously distort moveout velocity on conventional spreads close to the reflector depth.

An attractive feature of parameter estimation in HTI media is the possibility to find the true vertical velocity and reflector depth from  $P$ -wave moveout data. In contrast, surface data acquired over VTI and orthorhombic media do not provide enough information for the trans-

ition from moveout to vertical velocities. Therefore,  $P$ -wave moveout inversion for horizontal transverse isotropy allows one to build a velocity model for *depth* processing, as opposed to *time* processing in VTI and orthorhombic media.

Another advantage of the HTI model is a relatively simple relationship between the moveout parameters and the physical properties of crack systems. The direction of the symmetry axis yields the crack orientation, while the parameters  $\epsilon^{(V)}$  and  $\delta^{(V)}$  can be combined to estimate the shear-wave splitting coefficient  $\gamma^{(S)}$  and the crack density (Tsvankin, 1997). Furthermore, the relationship between  $\epsilon^{(V)}$ ,  $\delta^{(V)}$ , and the crack density depends on the contents of the cracks, which makes it possible to distinguish between fluid-filled and dry cracks using  $P$ -wave moveout data.

Although  $P$ -wave moveout in HTI media can provide us with a wealth of information, it is still beneficial to combine it with amplitude-variation-with-offset (AVO) signature or results of shear-wave splitting analysis. For instance,  $P$ -wave AVO gradient depends on a combination of  $\delta^{(V)}$  and  $\gamma^{(S)}$  (Rüger, 1996) and, therefore, can be used to evaluate the shear-wave splitting parameter. The coefficient  $\gamma^{(S)}$  can also be found directly by studying time delays between two split shear waves at vertical incidence. In addition, both the AVO response and shear-wave polarizations yield an independent estimate of the azimuth of the symmetry axis.

## Acknowledgments

This work was initiated during P. Contreras' visit to the Center for Wave Phenomena, Colorado School of Mines, in 1996. P. Contreras is grateful to INTEVEP S.A. for supporting his stay at CSM.

## References

- Al-Dajani, A., and Alkhalifah, T., 1997, Inversion of NMO velocity from horizontal reflectors in azimuthally anisotropic media: Accuracy and acquisition requirements: This volume.
- Al-Dajani, A., and Tsvankin, I., 1996, Nonhyperbolic reflection moveout for horizontal transverse isotropy: 66th Ann. Internat. Mtg., Soc. Expl. Geophys., Expanded Abstracts, 1495–1498 (also in CWP Project Review-96).
- Alkhalifah, T., and Tsvankin, I., 1995, Velocity analysis in transversely isotropic media: *Geophysics*, **60**, 1550–1566.
- Grechka, V., and Tsvankin, I., 1996, 3-D description of normal moveout in anisotropic media: 66th Ann. Internat. Mtg., Soc. Expl. Geophys., Expanded Abstracts, 1487–1490; also this volume.
- Grechka, V., and Tsvankin, I., 1997, Moveout velocity analysis and parameters estimation for orthorhombic media: this volume.
- Grechka, V., Tsvankin, I., and Cohen, J.K., 1997, Normal-moveout velocity and generalized Dix equation for inhomogeneous anisotropic media: submitted to *Geophysics*, also this volume.
- Rüger, A., 1996, Reflection coefficients and azimuthal AVO analysis in anisotropic media: PhD thesis, Colorado School of Mines.
- Schoenberg, M., and Helbig, K., 1997, Orthorhombic media: Modeling elastic wave behavior in a vertically fractured earth: *Geophysics*, in print.
- Thomsen, L., 1986, Weak elastic anisotropy: *Geophysics*, **51**, 1954–1966.
- Thomsen, L., 1988, Reflection seismology over azimuthally anisotropic media: *Geophysics*, **53**, 304–313.
- Thomsen, L., 1995, Elastic anisotropy due to aligned cracks in porous rock: *Geophysical Prospecting*, **43**, 805–830.
- Tsvankin, I., 1995, Normal moveout from dipping reflectors in anisotropic media: *Geophysics*, **60**, 268–284.
- Tsvankin, I., 1996, Effective parameters and  $P$ -wave velocity for azimuthally anisotropic media: 66th Ann. Internat. Mtg., Soc. Expl. Geophys., Expanded Abstracts, 1850–1853.
- Tsvankin, I., 1997, Reflection moveout and parameter estimation for horizontal transverse isotropy: *Geophysics*, **62**, 614–629.
- Wild, P., and Crampin, S., 1991, The range of effects of azimuthal isotropy and EDA anisotropy in sedimentary basins: *Geophys. J. Int.*, **107**, 513–529.

